# Stabilization effects of chemotaxis on bacterial aggregation patterns

**Ramón G. Plaza**
Institute of Applied Mathematics (IIMAS)
Universidad Nacional Autónoma de México

December 9, 2019

XII Americas Conference on Differential Equations. CIMAT, Guanajuato, December 9-13, 2019.

# Table of contents

# Nutrient taxis model with nonlinear cross-diffusion

# Bacterial (in vitro) dynamical patterns

- Bacterial colonies *in vitro* exhibit complex morphological aggregation patterns
- Hostile environmental conditions: low nutrient level, hard agar, presence of anti-biotics, etc.
- Adaptive survival strategies lead to complex spatio-temporal patterns.
- Complex self-organization: micro-level (cell-cell), macro-level (colony), chemical signalling, gene exchange, etc.

# Example: Bacillus subtilis

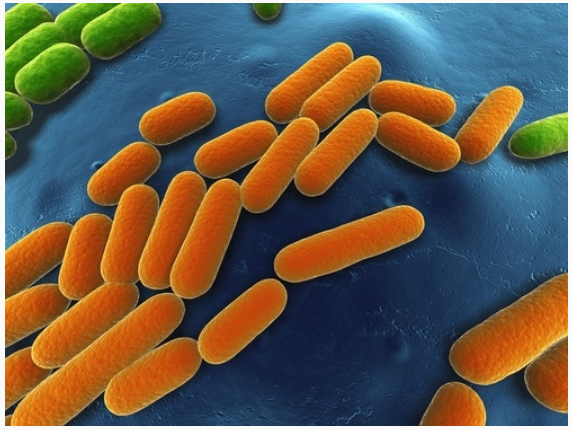

- Gram positive bacterium, rod-shaped, aerobe.
- Protective endospore (tolerate extreme environmental conditions)
- Very flagellated

# In vitro experiments (cf. Ohgiwari et al., 1992)

- Strain of *B. subtilis* point inoculated in center of Petri dish
- Agar plate containing peptone as nutrient
- Average pore size of the agar smaller that size of bacteria, inducing two-dimensional growth on agar surface

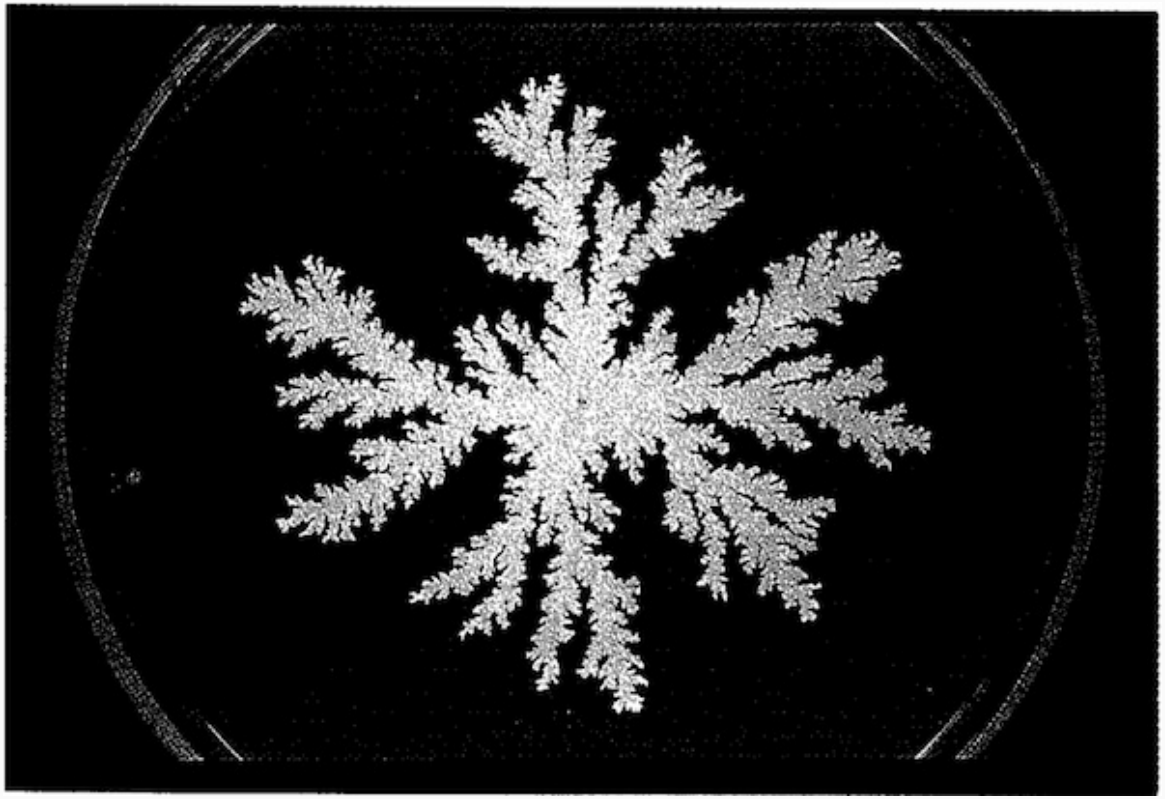

*Bacillis subtilis* strain on 0.75% of agar substrate. Fractal growth due to low level of nutrient. Courtesy of: Fujikawa, Matsushita, J. Phys. Soc. Japan (1989).

# Observations

- Low nutrient, hard agar: Diffusion limited aggregation (DLA). Fractal patterns (**Matsuyama and Matsushita (1993); Ben-Jacob (1994)**). **(A)**
- Semi-solid agar, low nutrient: Dense branch morphology (DBM). Smooth colony envelope (**Ohgiwari et al. (1992)**). **(E)**
- Higher nutrient, soft agar: homogeneous colony, smooth boundary envelope. **(D)**
- Hard agar, high nutrient: envelope with fractal boundary. **(B)**
- Rings: transition from **(B)** to **(D)**.

$C_v$ - concentration of nutrient; $C_a$ - agar concentration (softness $1/C_a$)

# Morphological diagram

Rings (C) Fractal (A)

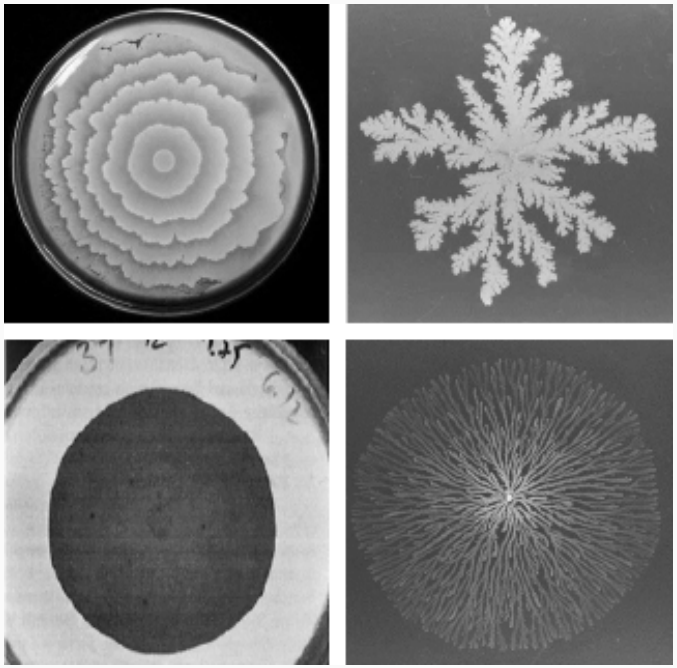

Disk (D) DBM (E)

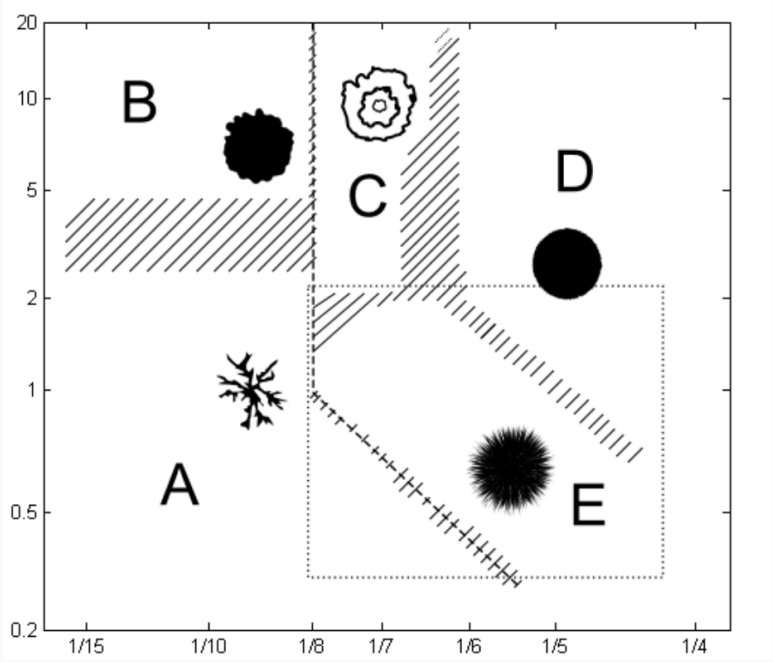


$C_v$ vs. $1/C_a$

# How to model the dynamics?

- **Bacteria as discrete agents:** Model bacteria as discrete self-propelled particles. Move, interact with environment. Agents consume nutrients, multiply, sporulate and die. Suitable to track the internal state of bacteria.
- **Bacteria as a continuous density:** Describe the evolution of bacterial concentration. Other constituents (nutrients, signaling factors, etc.) are also densities.

# Experimental observations

- **Ohgiwari et al. (1992)**:
  - In the DBM regime: movement of bacteria inactive in the inner region with low nutrient levels; active at the periphery with high nutrient
  - Cells become inactive again at the outermost front of bacterial colonies where cell density is apparently low
- **Ben-Jacob et al. (1994)**: Experimental evidence of chemotaxis of *B. subtilis* towards amino acids (nutrients)
- **Ben-Jacob et al. (2000)**: Identified three types of chemotactic internal signalling:
  - (Repulsive - Long range) By starving bacteria in the center.
  - (Attractive - Short range) Bacteria in the front ask for help to metabolize waste.
  - **Nutrient taxis:** Dominant signal. Attractive, short range.
- Proposed (**Ben-Jacob et al., 2000**), based on experiments, a relation bet. diffusion and chemotaxis (certain nutrient regimes).

# Chemotactic model with non-linear cross diffusion (i)

**Leyva, Málaga, P. Phys. A (2013)**. Model system in non-dimensional form:

$$\begin{aligned} v_t &= \Delta v - uv, \\ u_t &= \nabla \cdot (\sigma uv \nabla u) + uv - \chi_0 \nabla \cdot \left( \frac{\sigma v u^2}{(1+v)^2} \nabla v \right), \end{aligned} \tag{RDC}$$

$v$ - nutrient and $u$ - bacterial concentrations, $(x, y) \in \Omega \subset \mathbb{R}^2$, $t > 0$. $\Omega$ bounded, open set. Nutrient diffusion coefficient: $D_v \equiv 1$ constant. $\chi_0 > 0$ - constant (chemotactic sensitivity). $0 < \sigma \sim 1/C_a$ (constant) measures hardness of the agar.

# Chemotactic model with nonlinear cross-diffusion (ii)

System (RDC) is further endowed with:

- No-flux boundary conditions:

$$\nabla u \cdot \hat{n} = 0, \quad \nabla v \cdot \hat{n} = 0, \qquad (x, y) \in \partial\Omega, \;\; t > 0.$$

- Initial conditions:

$$u(x, y, 0) = u_0(x, y), \quad v(x, y, 0) = v_0(x, y), \qquad (x, y) \in \Omega.$$

# Modelling chemotaxis

General form of chemotactic term of **Keller-Segel (1971)**-type: add a term of form $\mathrm{div} J_c$, where

$$J_c = \zeta(u,v)\chi(v)\nabla v$$

$\chi = \chi(v) \gtrless 0$ - chemotactic sensitivity function; $\zeta = \zeta(u,v)$ - bacterial response function to nutrient gradient.

Ben-Jacob's experimental observation (**Ben-Jacob et al. (2000)**): In semi-solid agar, low colony density,

$$|\zeta(u,v)| \propto uD_u. \qquad (*)$$

Bacterial response function:

$$\zeta(u,v) = uD_u = \sigma u^2 v.$$

**Example:** if the diffusion coefficient is constant, $D > 0$, then we recover the classical Keller-Segel chemotactic flux, $J_c = \pm\chi u\nabla v$

# Modelling chemotaxis

General form of chemotactic term of **Keller-Segel (1971)**-type: add a term of form $\mathrm{div} J_c$, where

$$J_c = \zeta(u,v)\chi(v)\nabla v$$

$\chi = \chi(v) \gtrless 0$ - chemotactic sensitivity function; $\zeta = \zeta(u,v)$ - bacterial response function to nutrient gradient.

Ben-Jacob's experimental observation (**Ben-Jacob et al. (2000)**): In semi-solid agar, low colony density,

$$|\zeta(u,v)| \propto uD_u. \qquad (*)$$

Bacterial response function:

$$\zeta(u,v) = uD_u = \sigma u^2 v.$$

**Example:** if the diffusion coefficient is constant, $D > 0$, then we recover the classical Keller-Segel chemotactic flux, $J_c = \pm\chi u\nabla v$

**Note:** This relationship can be theoretically justified by taking a diffusive limit of a stochastic velocity jump process: **P., J. Math. Biol. (2019)**

# Features:

- Nonlinear degenerate cross-diffusion (**Kawasaki et al. (1997)**): $D_u = \sigma uv$.
- Conveys immotility when either *u or v* are low. Models high activity in the boundary only.
- Valid for the transition region **E** $\leftrightarrow$ **D**
- Complex dense morphology
- Chemotactic sensitivity: **Lapidus-Schiller (1976)** receptor's law (attractive),

$$\chi(v) = -\frac{\chi_0}{(1+v)^2}, \quad \chi_0 > 0.$$

- Kinetic (production/consumption) term $f(u, v) = \pm uv$
- Rich mathematical structure (**Satnoianu, Maini and Sánchez-Garduño (2001); Sherratt (2010)**).

# Numerical simulations

- Square domain $[0,1] \times [0,1]$. Grid of $2048 \times 2048$
- Finite difference, 2nd. order Runge-Kutta scheme
- Very small time steps to avoid instabilities (stiffness)
- Crudeness of the scheme compensated by parallel high performance computations with Graphic Processing Units (GPUs)
- Millions of steps in a few hours.
- NVIDIA Tesla© C2070 graphics card with 448 CUDA cores


- Initial conditions:

$$v(x,y,0) \equiv \overline{v}_0, \quad u(x,y,0) = 0.71\, e^{-(x^2+y^2)/6.25} \text{ (Kawasaki)}$$

- Parameter values: $\sigma = 4.0$ (soft-medium agar); $\overline{v}_0 = 0.71$ (initial constant nutrient concentration); chemotactic signal $\chi_0 = 0, 2.5, 5.0$.

# No chemotaxis: $\chi_0 = 0$

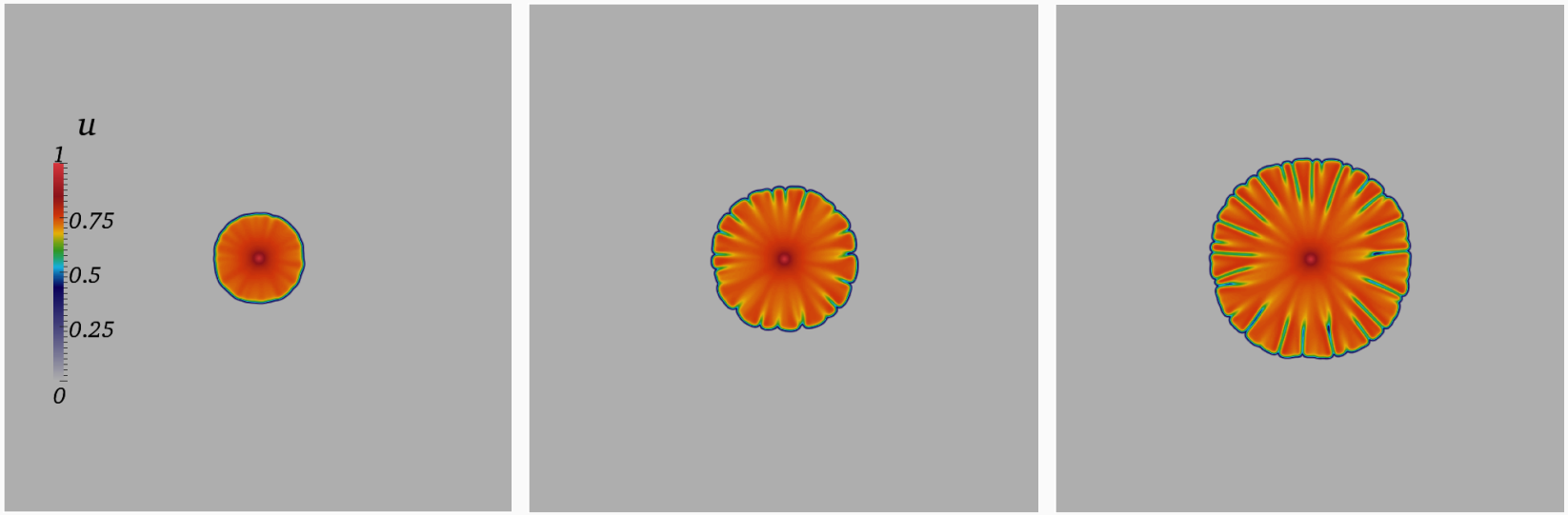


$t \sim 5\,\text{min.}$ $t \sim 10\,\text{min.}$ $t \sim 15\,\text{min.}$

# $\chi_0 = 2.5$

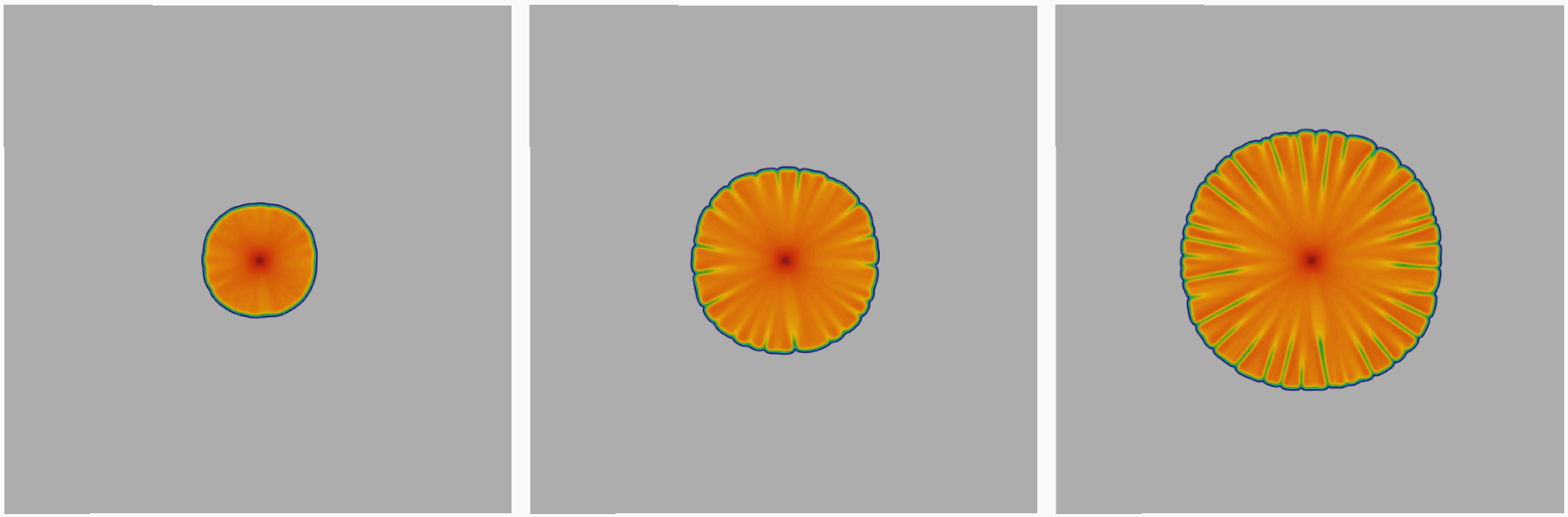

$t \sim 5\,\text{min.}$ $t \sim 10\,\text{min.}$ $t \sim 15\,\text{min.}$

# $\chi_0 = 5.0$

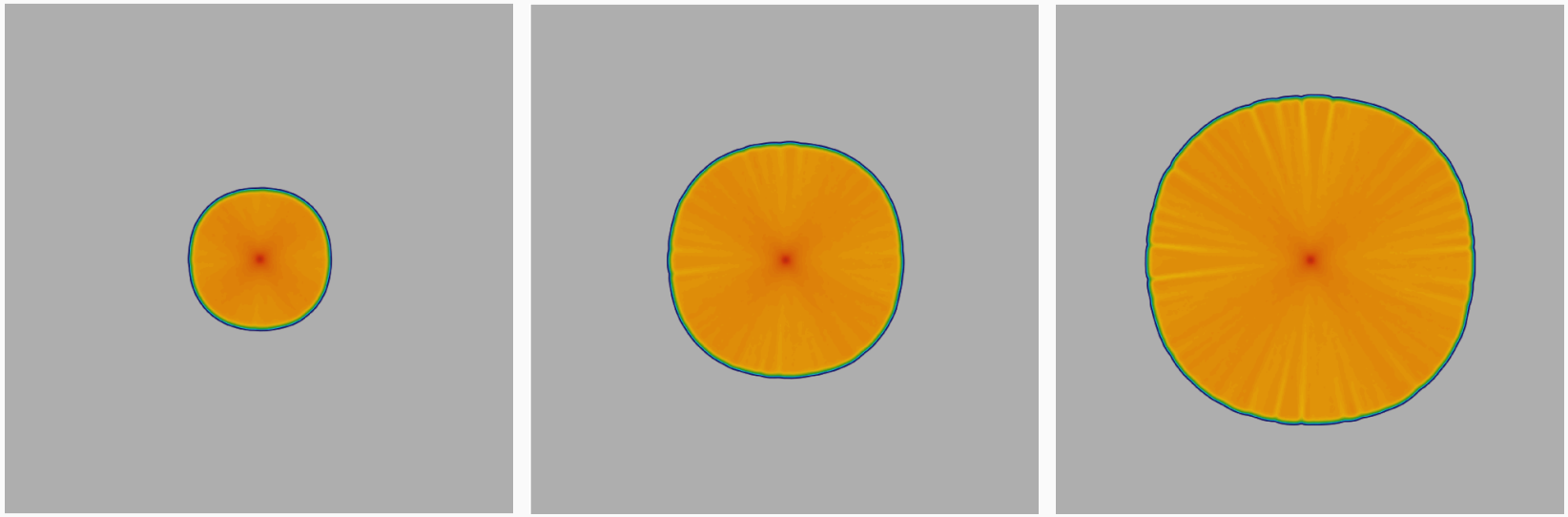

$t \sim 5\,\text{min.}$ $t \sim 10\,\text{min.}$ $t \sim 15\,\text{min.}$

# Main results (i): Leyva, Málaga, P. (2013)

- Incorporation of a suitable chemotactic term to Kawasaki's nonlinear cross diffusion model, compatible with low-nutrient regime experimental observations (Ben-Jacob)
- High resolution numerical simulations confirm enhancement of the speed
- Numerical observation: In the low-nutrient, soft-agar regime: change in morphology, patterns become smoother (less branches) in the presence of chemotaxis
- Numerical estimation (one-d simulation) approximates well the asymptotic speed calculation
- Under the conservation law approximation, the front equation becomes a scalar reaction-diffusion equation with degenerate diffusion
- Asymptotics show that the speed of the envelope front increases with chemotaxis

# Main results (ii): Butanda, Málaga, P. (2017)

- The change in morphology in the DBM regime can be explained and quantified
- Asymptotics: quantitative analysis shows that when the chemotactic sensitivity is increased, the eigenvalues of the linearized operator around the envelope front become "more stable"
- Energy estimates provide bounds for the eigenvalues of the linearized operator around the front. These bounds decrease as functions of the chemotactic sensitivity $\chi_0 \geq 0$, suggesting that, the patterns become more stable

# The stabilizing effect of chemotaxis: a traveling front approach

# Model system and hypotheses

**Generic model system:**

$$u_t = \nabla \cdot \left(\bar{D}(u,v)\nabla u\right) - \nabla \cdot \left(\xi(u,v)\chi(v)\nabla v\right) + uv,$$
$$v_t = \Delta v - uv,$$

$(x,y) \in \Omega \subset \mathbb{R}^2$, $t > 0$, + Neumann b.c. and initial cond.

**Hypotheses:**

(H1) $\bar{D} \in C^2(\mathbb{R}^2)$, $\bar{D}(u,v) \geq 0$ for all $u, v \in \mathbb{R}$. Moreover, $\bar{D} = 0$ if $u = 0$ or $v = 0$.

(H2) For all $u, v \in \mathbb{R}$ under consideration:

$$\xi(u,v) = u\bar{D}(u,v).$$

(H3) $\chi \in C^2(\mathbb{R})$ and uniformly bounded: $0 \leq \chi(v) \leq C$ for some constant $C > 0$ and all $v \in \mathbb{R}$.

# Approximations (i)

**First approximation**: due to balanced production/loss terms $\pm uv$, in the absence of diffusion and chemotaxis the total mass is conserved (**Kawasaki et al. (1997)**). Thus, in the DBM regime and for small values of $u$ and $v$ there holds

$$u + v \approx C, \quad \text{constant.}$$

Choose $C = v_0$ (nutrient reference value):

$$v = v_0 - u.$$

# Approximations (ii)

Upon substitution, scalar equation for the bacterial density $u$

$$u_t = \nabla \cdot \big(D(u)\nabla u\big) + g(u), \qquad (x,y) \in \Omega, \quad t > 0.$$

Effective nonlinear, doubly-degenerate, density-dependent diffusion coefficient:

$$D(u) := \bar{D}(u, v_0 - u)\big(1 + u\chi(v_0 - u)\big).$$

Effective reaction term:

$$g(u) := v_0 u\left(1 - \frac{u}{v_0}\right).$$

# Approximations (ii)

Upon substitution, scalar equation for the bacterial density $u$

$$u_t = \nabla \cdot \big(D(u)\nabla u\big) + g(u), \qquad (x,y) \in \Omega, \quad t > 0.$$

Effective nonlinear, doubly-degenerate, density-dependent diffusion coefficient:

$$D(u) := \bar{D}(u, v_0 - u)\big(1 + u\chi(v_0 - u)\big).$$

Effective reaction term:

$$g(u) := v_0 u\left(1 - \frac{u}{v_0}\right).$$

**Remark:** The chemotactic term has been absorbed into the new nonlinear diffusion.

# Approximations (iii)

**Second approximation**: Geometric front propagation

- Local curvilinear coordinates: normal $\zeta(x, y, t)$, tangent $\tau(x, y, t)$
- $u(x, y, t) \approx u(\zeta(x, y, t))$ motion in the normal direction

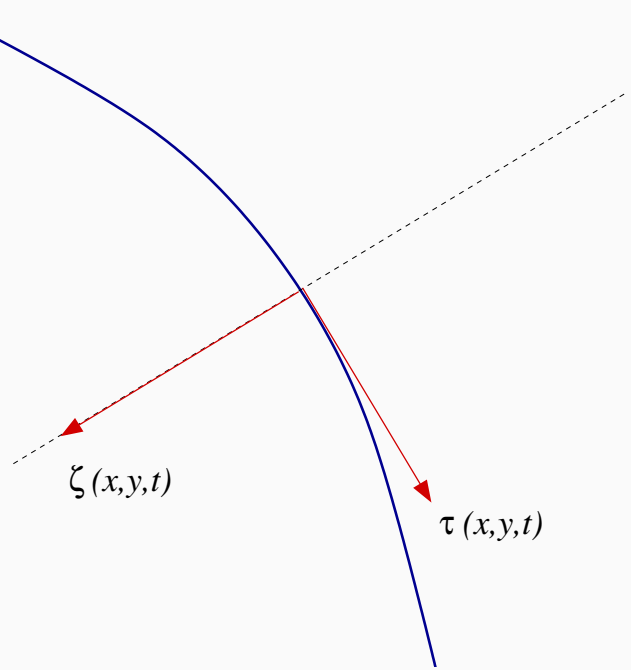


Making a rotation of coordinates we assume $u(x, y, t) \approx \phi(x - ct)$, front propagates in the $x$-direction.

# Approximations (iv)

**Third approximation**: approximate $\chi(v)$ by a constant value,

$$\chi(v) \equiv \chi(0) = \chi_0 \geq 0,$$

For suitably normalized values of $v \in [0, v_0]$ the Lapidus-Schiller chemotactic law is uniformly bounded: this approximation represents no loss of generality.

# Envelope front (i)

**Ansatz**: one-dimensional planar front solution of the form

$$u(x, y, t) = \phi(x - ct) = \phi(z),$$

on a strip domain,

$$\Omega_L = \{(x, y) \in \mathbb{R}^2 : -\infty < x < \infty,\ 0 < y < L\},$$

some $L > 0$. $z := x - ct$, $c \in \mathbb{R}$ constant speed.

Substituting we obtain the profile ODE

$$-c\phi_z = D(\phi)\phi_{zz} + D(\phi)_z\phi_z + g(\phi).$$

# Envelope front (ii)

In pattern formation problems, it is natural to consider infinite domains and to neglect the influence of boundary conditions. Due to finite speed of propagation and the fact that we are interested in the local-in-time, local-in-space evolution near the interface this means no loss of generality.

Consequently, we assume that the front has asymptotic limits of the form

$$u_{\pm} = \lim_{z \to \pm\infty} \phi(z).$$

The front spreads from the region occupied by the cells toward outer regions filled with nutrient. Hence:

$$u_{+} = 0, \qquad u_{-} = v_0.$$

Moreover, the front is monotone:

$$\phi_z(z) < 0, \qquad \text{for all } z \in \mathbb{R}.$$

# Existence theory (i)

**Theoretical results**

- **Malaguti and Marcelli (2003)**

Fisher-KPP equation with doubly degenerate diffusion:

$$u_t = (D(u)u_x)_x + g(u)$$

$0 < u < 1$, $D \in C^1([0,1])$, $g \in C^1([0,1])$

$$D(0) = D(1) = 0, \qquad D(u) > 0 \ \text{ for all } \ 0 < u < 1,$$
$$g(0) = g(1) = 0, \qquad g(u) > 0 \ \text{ for all } \ 0 < u < 1,$$

# Existence theory (ii)

Malaguti and Marcelli show existence of monotone TWS provided the speed $c$ satisfies:

$$0 < c_* \leq c$$

Threshold velocity $c_*$ of a sharp front:

$$0 < c_* \leq 2\sqrt{\sup_{s\in(0,1)} \frac{D(s)g(s)}{s}}.$$

# Existence theory (iii)

By-products of existence results:

- Heteroclinic orbit belongs to a center manifold passing through degenerate equilibria; e.g. when $\phi(z) \to 0$ as $z \to +\infty$,

$$\phi_z = -\alpha\phi + O(\phi^2) < 0, \quad \text{(monotone)}$$

for some $\alpha > 0$; we deduce exponential decay of $\phi$ and derivatives,

$$|\phi|, |\phi_z|, |\phi_{zz}| \leq Ce^{-\alpha z}, \quad z \to +\infty,$$

- Degenerate diffusion coefficients decay exponentially to zero as they approach equilibria,

$$D(\phi) \to 0, \text{ as } \phi(z) \to \begin{cases} 0, & z \to +\infty \\ v_0, & z \to -\infty, \end{cases}$$

# Perturbation of the envelope front

Consider perturbations of form $w = w(z, y, t)$ with b.c.

$$\left.\begin{aligned} w(\pm\infty, y, t) = 0, \qquad & t > 0,\ 0 < y < L, \\ w(z, L, t) = w(z, 0, t) = 0, \qquad & t > 0,\ z \in \mathbb{R}. \end{aligned}\right\}$$

Substituting $u(x, y, t) = \phi(z) + w(z, y, t)$ and linearizing around the front:

$$w_t = D(\phi)\big(w_{zz} + w_{yy}\big) + \big(2D(\phi)_z + c\big)w_z + \big(D(\phi)_{zz} + g'(\phi)\big)w.$$

# Spectral stability problem

Consider perturbations of form

$$w(z,y,t) = e^{\lambda t} U(z,y),$$

$\lambda \in \mathbb{C}$, $U \in L^2(\Omega_L)$, with b.c.

$$\left.\begin{aligned} U(\pm\infty, y) &= 0, \qquad & y &\in [0,L], \\ U_y(z,0) = U_y(z,L) &= 0, & z &\in \mathbb{R}. \end{aligned}\right\}$$

Upon substitution we get the spectral problem

$$\lambda U = D(\phi)\big(U_{zz} + U_{yy}\big) + \big(2D(\phi)_z + c\big)U_z + \big(D(\phi)_{zz} + g'(\phi)\big)U,$$

RHS defines a closed, densely defined operator in $L^2(\Omega_L)$

$$\mathscr{L}U := D(\phi)\big(U_{zz} + U_{yy}\big) + \big(2D(\phi)_z + c\big)U_z + \big(D(\phi)_{zz} + g'(\phi)\big)U,$$
$$\mathscr{L} : \mathscr{D}(\mathscr{L}) = H^2(\Omega_L) \subset L^2(\Omega_L) \to L^2(\Omega_L),$$

with domain $\mathscr{D}(\mathscr{L}) = H^2(\Omega_L)$. $\lambda$ - eigenvalue, $U$ - eigenfunction.

# Eigenfunction decomposition (i)

For any $U \in H^2(\Omega_L)$ eigenfunction and any $m = 0, 1, 2, \ldots$, define

$$U_m(z) := \int_0^L U(z,y)\, Y_m(y)\, dy,$$

where

$$Y_m(y) = \begin{cases} \dfrac{1}{\sqrt{L}}, & m = 0, \\ \sqrt{\dfrac{2}{L}} \cos\left(\dfrac{m\pi y}{L}\right), & m = 1, 2, \ldots \end{cases}$$

Eigenfunctions are thus decomposed as

$$U(z,y) = \sum_{m=0}^{+\infty} U_m(z)\, Y_m(y).$$

# Eigenfunction decomposition (ii)

**Hierarchy of spectral equations**

For each $m \in \mathbb{Z}$, $m \geq 0$,

$$\lambda U_0 = D(\phi)\partial_z^2 U_0 + \big(2D(\phi)_z + c\big)\partial_z U_0 + \big(D(\phi)_{zz} + g'(\phi)\big) U_0, \quad \text{for } m = 0,$$

and,

$$\lambda U_m = D(\phi)\partial_z^2 U_m + \big(2D(\phi)_z + c\big)\partial_z U_m + \left(D(\phi)_{zz} + g'(\phi) - \frac{m^2\pi^2}{L^2} D(\phi)\right) U_m,$$

for the same eigenvalue $\lambda \in \mathbb{C}$

# Traslation invariance

The function $\Phi := \phi_z \in H^2(\mathbb{R})$ is a solution with $\lambda = 0$ and $m = 0$.
Differentiate profile equation:

$$0 = D(\phi)\Phi_{zz} + \big(2D(\phi)_z + c\big)\Phi_z + \big(D(\phi)_{zz} + g'(\phi)\big)\Phi.$$

$\lambda = 0$ - eigenvalue associated to translation invariance, with eigenfunction $U(z, y) = \Phi(z) = \phi_z(z)$. Expansion is given by $U_0 = \sqrt{L}\phi_z$, and

$$U_m(z) = \int_0^L \phi_z(z) Y_m(y)\, dy = 0,$$

for all $m \geq 1$.

# Energy estimates and transversal stability (i)

For each $m \in \mathbb{Z}$, $m \geq 0$, define

$$W_m(z) := U_m(z) \exp\left(\frac{c}{2}\int_{z_0}^{z} \frac{d\zeta}{D(\phi(\zeta))}\right),$$

where $z_0 \in \mathbb{R}$ is fixed but arbitrary.

**Lemma** *From exponential decay of the eigenfunction $U \in H^2(\Omega_L)$ we have for each $m \geq 1$*

$$W_m \in H^2(\mathbb{R}).$$

Upon substitution:

$$\lambda W_m = D(\phi)\partial_z^2 W_m + 2D(\phi)_z \partial_z W_m + \left(H(z) - \frac{m^2}{\pi^2 L^2} D(\phi)\right) W_m,$$

$$H(z) := D(\phi)_{zz} + g'(\phi) - \frac{c^2}{4D(\phi)} - \frac{cD(\phi)_z}{2D(\phi)}.$$

# Energy estimates and transversal stability (ii)

**Lemma (spectral transversal stability)**
*If $\lambda \in \mathbb{C}$ is an eigenvalue of the associated spectral problem, such that last equation holds for each mode $m \in \mathbb{Z}$, $m \geq 0$ with $W_m \in H^2(\mathbb{R})$, then $\lambda \in \mathbb{R}$ and $\lambda \leq 0$.*

**Proof sketch:** When $m = 0$ and $\Phi = \phi_z$, the change of variables for this eigenfunction

$$\Psi(z) := \Phi(z) \exp\Big(\frac{c}{2} \int_{z_0}^{z} \frac{d\zeta}{D(\phi(\zeta))}\Big),$$

yields

$$0 = D(\phi)\partial_z^2 \Psi + 2D(\phi)_z \partial_z \Psi + H(z)\Psi.$$

Multiply both eqs. by $D(\phi) \geq 0$ and rearrange the terms:

$$\lambda D(\phi) W_m = \partial_z \big(D(\phi)^2 \partial_z W_m\big) + D(\phi) H(z) W_m - \frac{m^2}{\pi^2 L^2} D(\phi)^2 W_m, \quad (*)$$

$$0 = \partial_z \big(D(\phi)^2 \Psi_z\big) + D(\phi) H(z) \Psi. \quad (**)$$

# Energy estimates and transversal stability (iii)

Substitute

$$D(\phi)H(z) = -\frac{(D(\phi)^2\Psi_z)_z}{\Psi},$$

into (**??**) to arrive at

$$\lambda D(\phi)W_m = \left(D(\phi)^2\partial_z W_m\right)_z - \left(\frac{D(\phi)^2\Psi_z}{\Psi} + \frac{m^2}{\pi^2 L^2}D(\phi)^2\right)W_m.$$

Take the $L^2$ product of $W_m$ with last equation and integrate by parts:

$$\begin{aligned}
\lambda\int_{-\infty}^{+\infty} D(\phi)|W_m|^2\,dz &= \int_{-\infty}^{+\infty}\bar{W}_m(D(\phi)^2\partial_z W_m)_z\,dz - \int_{-\infty}^{+\infty}\frac{(D(\phi)^2\Psi_z)_z}{\Psi}|W_m|^2\,dz + \\
&\quad - \frac{m^2}{\pi^2 L^2}\int_{-\infty}^{+\infty} D(\phi)^2|W_m|^2\,dz \\
&= \int_{-\infty}^{+\infty} D(\phi)^2\left(\Psi_z\partial_z\left(\frac{|W_m|^2}{\Psi}\right) - |\partial_z W_m|^2 - \frac{m^2}{\pi^2 L^2}|W_m|^2\right)dz \\
&= -\int_{-\infty}^{+\infty} D(\phi)^2\Psi^2\left|\partial_z\left(\frac{W_m}{\Psi}\right)\right|^2 dz - \frac{m^2}{\pi^2 L^2}\int_{-\infty}^{+\infty} D(\phi)^2|W_m|^2\,dz \\
&\leq 0,
\end{aligned}$$

for any $m \geq 1$. We conclude that $\lambda$ is real and non-positive. □

# Remark

- At first order approximation (locally planar front for a scalar equation due to the balanced source and loss kinetic terms), the envelope front is stable under transversal small, local-in-space perturbations. This behavior is verified by numerics on the actual (curved) envelope front.

# The stabilizing effect of chemotaxis (i)

**Weighted Sobolev spaces**

Define

$$\eta(z) := \sqrt{D(\phi(z))} \geq 0, \qquad z \in \mathbb{R}.$$

Customary weighted energy function spaces

$$H^k_\eta(\mathbb{R};\mathbb{C}) = \{v : \eta(z)v(z) \in H^k(\mathbb{R};\mathbb{C})\},$$

for $k \in \mathbb{Z}$, $k \geq 0$, which are Hilbert spaces endowed with the inner product (and norm),

$$\langle u, v\rangle_{H^k_\eta} := \langle \eta\, u, \eta\, v\rangle_{H^k}, \qquad \|v\|^2_{H^k_\eta} := \|\eta\, v\|^2_{H^k} = \langle v, v\rangle_{H^k_\eta}.$$

According to custom: $H^0_\eta(\mathbb{R};\mathbb{C}) = L^2_\eta(\mathbb{R};\mathbb{C})$.

# The stabilizing effect of chemotaxis (ii)

Let $\lambda \in (-\infty, 0]$ be an eigenvalue associated to an eigenfunction $U = \sum U_m Y_m \in H^2(\Omega_L)$. Let $m \in \mathbb{Z}$, $m \geq 1$ be a single mode for which $U_m \not\equiv 0$. Consequently, $W_m \not\equiv 0$ and $\|W_m\|_{L^2_\eta} > 0$. (The modes $m \geq 1$ for which $U_m \equiv 0$ do not contribute to the energy estimate.) Then

$$|\lambda| \int_{-\infty}^{+\infty} D(\phi)|W_m|^2\,dz = \int_{-\infty}^{+\infty} D(\phi)^2 |\partial_z W_m|^2\,dz + \frac{m^2}{\pi^2 L^2} \int_{-\infty}^{+\infty} D(\phi)^2 |W_m|^2\,dz + J,$$

where

$$J := -\int_{-\infty}^{+\infty} D(\phi)^2 \Psi_z \partial_z \left( \frac{|W_m|^2}{\Psi} \right) dz = \int_{-\infty}^{+\infty} 2D(\phi) D'(\phi) \phi_z \frac{\Psi_z}{\Psi} |W_m|^2\,dz + \int_{-\infty}^{+\infty} D(\phi)^2 \frac{\Psi_{zz}}{\Psi} |W_m|^2\,dz.$$

# The stabilizing effect of chemotaxis (ii)

Let $\lambda \in (-\infty, 0]$ be an eigenvalue associated to an eigenfunction $U = \sum U_m Y_m \in H^2(\Omega_L)$. Let $m \in \mathbb{Z}$, $m \geq 1$ be a single mode for which $U_m \not\equiv 0$. Consequently, $W_m \not\equiv 0$ and $\|W_m\|_{L^2_\eta} > 0$. (The modes $m \geq 1$ for which $U_m \equiv 0$ do not contribute to the energy estimate.) Then

$$|\lambda| \int_{-\infty}^{+\infty} D(\phi)|W_m|^2\,dz = \int_{-\infty}^{+\infty} D(\phi)^2 |\partial_z W_m|^2\,dz + \frac{m^2}{\pi^2 L^2} \int_{-\infty}^{+\infty} D(\phi)^2 |W_m|^2\,dz + J,$$

where

$$J := -\int_{-\infty}^{+\infty} D(\phi)^2 \Psi_z \partial_z \left( \frac{|W_m|^2}{\Psi} \right) dz = \int_{-\infty}^{+\infty} 2D(\phi)D'(\phi)\phi_z \frac{\Psi_z}{\Psi} |W_m|^2\,dz + \int_{-\infty}^{+\infty} D(\phi)^2 \frac{\Psi_{zz}}{\Psi} |W_m|^2\,dz.$$

**Lemma**
*The functions $D'(\phi)\phi_z \Psi_z/\Psi$ and $D(\phi)\Psi_{zz}/\Psi$ are uniformly bounded in $z \in \mathbb{R}$.*

**Proof.** Follows from the definition of $\Psi$, the exponential rates of decay and straightforward computations. □

# The stabilizing effect of chemotaxis (iii)

In view of last lemma:

$$|J| \leq C \int_{-\infty}^{+\infty} D(\phi)|W_m|^2 \, dz = C\|W_m\|^2_{L^2_\eta},$$

for some uniform $C > 0$. Substituting back yields:

$$|\lambda|\|W_m\|^2_{L^2_\eta} \leq \left(\sup_{z\in\mathbb{R}} D(\phi)\right)\left(\|\partial_z W_m\|^2_{L^2_\eta} + \frac{m^2}{\pi^2 L^2}\|W_m\|^2_{L^2_\eta}\right) + C\|W_m\|^2_{L^2_\eta}.$$

# The stabilizing effect of chemotaxis (iii)

In view of last lemma:

$$|J| \leq C \int_{-\infty}^{+\infty} D(\phi)|W_m|^2\, dz = C\|W_m\|^2_{L^2_\eta},$$

for some uniform $C > 0$. Substituting back yields:

$$|\lambda|\|W_m\|^2_{L^2_\eta} \leq \big(\sup_{z\in\mathbb{R}} D(\phi)\big)\left(\|\partial_z W_m\|^2_{L^2_\eta} + \frac{m^2}{\pi^2 L^2}\|W_m\|^2_{L^2_\eta}\right) + C\|W_m\|^2_{L^2_\eta}.$$

This estimate provides an upper bound for $|\lambda|$ in terms of each $m \geq 1$. Since $D(\phi)$ (weight of the Sobolev norm) depends on $\chi_0$ , normalize with respect to the weighted $L^2$-norm to obtain

$$|\lambda| \leq \rho_m C_m \big(\sup_{z\in\mathbb{R}} D(\phi)\big) + C,$$

where $\rho_m := \|W_m\|^2_{H^1_\eta}/\|W_m\|^2_{L^2_\eta} > 0$, $C_m > 0$ constant satisfying $C_m \leq C(1+m^2)$.

# The stabilizing effect of chemotaxis (iv)

**Lemma**
*For any $u \in H^1_\eta(\mathbb{R};\mathbb{C})$ with $\|u\|_{L^2_\eta} > 0$, the ratio*

$$\rho = \frac{\|u\|^2_{H^1_\eta}}{\|u\|^2_{L^2_\eta}}$$

*is a uniformly bounded function of $\chi_0 > 0$.*

**Proof:** Since $D(\cdot)$ is uniformly bounded from above, it is clear that $H^k_\eta \subset H^k$ for all $k \geq 0$. The conclusion follows by noticing that both the numerator and the denominator are linear on $\chi_0$,

$$\rho = \frac{\|u\|^2_{H^1_{\eta_1}} + \chi_0 \|u\|^2_{H^2_{\eta_2}}}{\|u\|^2_{L^2_{\eta_1}} + \chi_0 \|u\|^2_{L^2_{\eta_2}}} = O(1),$$

for all $\chi_0 > 0$ and where the weight functions $\eta_1, \eta_2$ are given by

$$\eta_1 = \sqrt{\sigma_0 v_0 \phi (1 - \phi/v_0)}, \quad \eta_2 = \sqrt{\sigma_0 v_0 \phi^2 (1 - \phi/v_0)}.$$

□

# The stabilizing effect of chemotaxis (v)

**Consequences:** the bounds for the eigenvalues and their dependence on the intensity of the chemotactic signal are controlled by

$$\sup_{z\in\mathbb{R}} D(\phi) = \max_{u\in[0,v_0]} D(u) = \max_{u\in[0,v_0]} \Big(\sigma_0 v_0 u\big(1-\frac{u}{v_0}\big)(1+\chi_0 u)\Big).$$

Let

$$G(u) := u\big(1-\frac{u}{v_0}\big)(1+\chi_0 u), \qquad u\in[0,v_0].$$

For positive values of $\chi_0 > 0$, the maximum $G$ on $[0,v_0]$ occurs at

$$u_*(v_0,\chi_0) = \frac{1}{3}\left(v_0 - \frac{1}{\chi_0} + \sqrt{\Big(v_0-\frac{1}{\chi_0}\Big)^2 + \frac{3v_0}{\chi_0}}\right) \in (0,v_0).$$

# The stabilizing effect of chemotaxis (vi)

Thus, the maximum of $G$ (and hence the energy bound for $|\lambda|$) is controlled by

$$\Theta(v_0, \chi_0) := G(u_*(v_0, \chi_0)) = u_*(v_0, \chi_0)\Big(1 - \frac{u_*(v_0, \chi_0)}{v_0}\Big)(1 + \chi_0 u_*(v_0, \chi_0)).$$

For fixed values of the initial nutrient concentration $v_0$, the bound $\Theta$ is an increasing function of the chemotactic signal $\chi_0 \geq 0$.

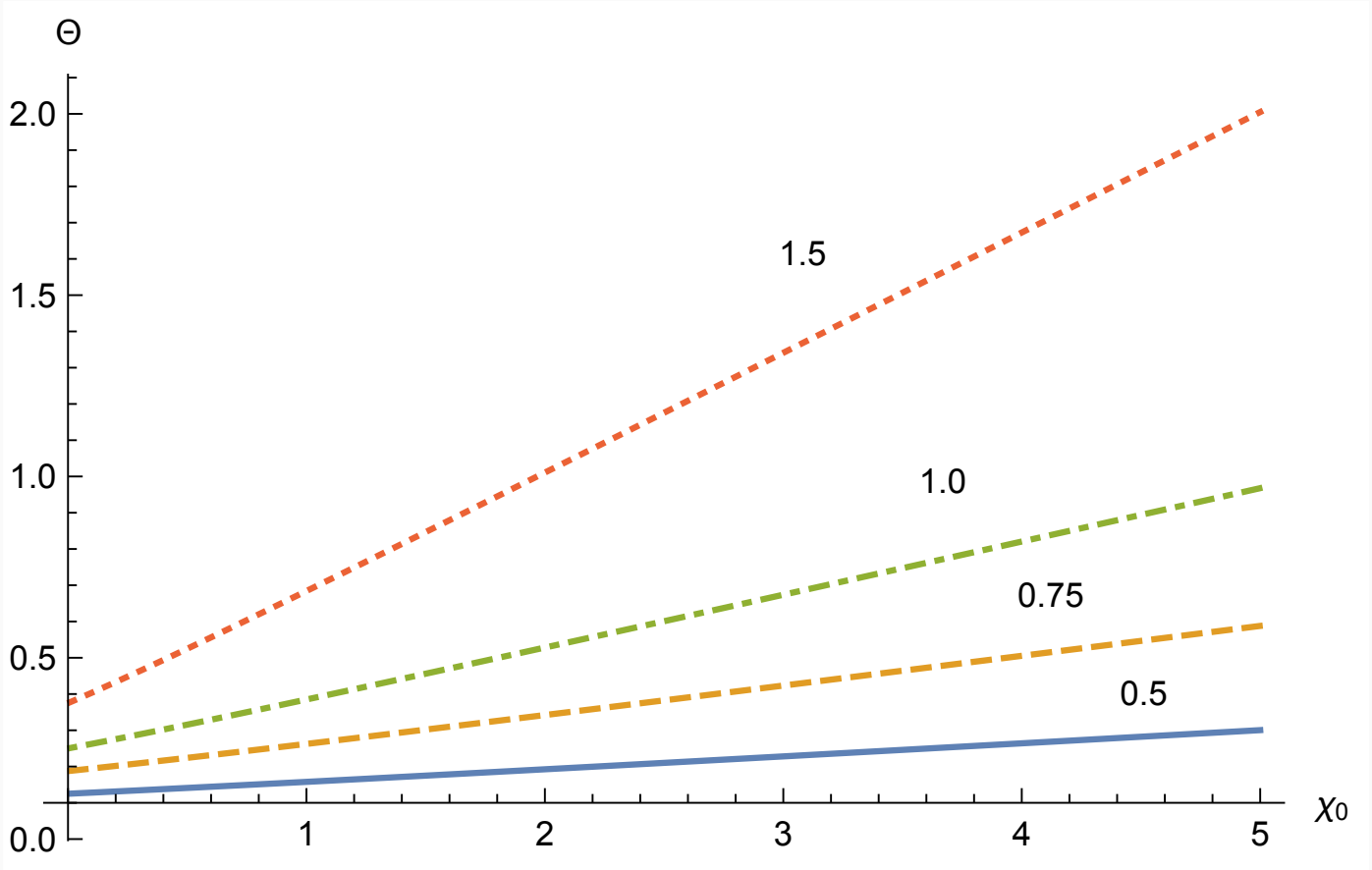


Behavior of $\Theta$ as a function of $\chi_0$, for different fixed values of $v_0 = 0.5, 0.75, 1.0, 1.5$.

# Discussion

# Discussion (i)

- Under balanced kinetic terms and the geometric front propagation approximation, the bacterial envelope fronts are spectrally stable under transversal perturbations.
- Energy estimates provide, in addition, bounds for the eigenvalues of the linearized operator around the front, which decrease as functions of the chemotactic sensitivity $\chi_0 \geq 0$, suggesting that, as $\chi_0$ grows, the patterns are "more stable".
- Heuristic explanation: the effective nonlinear density-dependent diffusion coefficient depends also on $\chi_0$, hence pushing the interface to be deformable on shorter scales than the new diffusion length as the chemotactic signal is increased.
- This quantitative observation is compatible with the results of **Arouh and Levine (2000)**: chemotaxis suppresses the instability of fronts for a Kessler-Levine system with constant diffusivities, nutrient chemotactic terms and balanced kinetic terms.

# Discussion (ii)

- **Tucker (2010)**: same observation for a model for *Paenibacillus dendritiformis*, also with balanced kinetic terms.
- In summary: supression of colony branching when the bacteria are assisted chemotactically toward nutrients.
- **Funaki, Mimura, Tsujikawa (2006)** show that when the chemotactic signal is present traveling front solutions are destabilized for a reaction-diffusion-chemotaxis system for which the production and degradation terms are not balanced.
- In systems without chemotaxis it is well-known that balanced kinetic terms cause stable wave pinning (**Mori, Jilkine, Edelstein-Keshet (2011)**.
- Loss of balabced form may cause branching instabilities.

**Thanks!**